Pettigrew, T.L., Casey, J.F., Miller, D.J., et al., 1999
Proceedings of the Ocean Drilling Program, Initial Reports Volume 179

5. NERO Site (1107)[1]

Shipboard Scientific Party[2]

THE NERO PROJECT

Introduction

Seismic data from a World-Wide Standardized Seismograph Network, established in the early 1960s, accelerated advances in seismology and were a great resource of new discoveries up to the 1970s. During the past 10 yr, our knowledge of the processes of the deep Earth has been greatly improved by the development of new generations of global monitoring networks in seismology and geodesy and by the continuation of long-term observations in geomagnetism (i.e., GEOSCOPE [a project that is run by the Institut de Physique du Globe de Paris], IRIS [Incorporated Research Institutions for Seismology], GeoFon [GEOForschungsNetz; a geophysical research network] on a global scale; and MedNet [MEDiterranean NETwork], Poseidon, CDSN [China Digital Seismic Network], GRSN [German Regional Seismic Network] on a regional scale). Although the quantity and quality of data have increased, this new information has revealed that there are large departures from lateral homogeneity at every level from the Earth's surface to its center. The intensive use of broadband data has provided remarkable seismic tomographic images of the Earth's interior. These models are now routinely used in geodynamics for earthquake studies and to obtain the complex time histories of the inhomogeneous earthquake faulting related to tectonics. Improvements in the observatory locations for seismology, geodesy, and geomagnetics, particularly in the oceans, can greatly enhance our understanding of the Earth's interior.

The observatory planned for the Ninetyeast Ridge will be part of the future network of seafloor observatories proposed in the International Ocean Network (ION) program. The selected site on the Ninetyeast Ridge (Fig. **F1;** Site 1107) was chosen because there was no expectation of any technical problems, as previous holes in this area were drilled

F1. Site map in the eastern Indian Ocean showing the location of Ninetyeast Ridge and NERO Site 1107, **p. 15.**

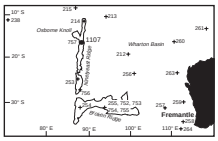

[1]**Examples of how to reference the whole or part of this volume.**
[2]**Shipboard Scientific Party addresses.**

Ms 179IR-105

with a single bit. The site chosen was Site 757 (Fig. F1), which was drilled during Leg 121 in 1988 (Peirce, Weissel, et al., 1989). Installing a reentry cone and casing down to basement was the first step toward the installation of a geophysical ocean-bottom observatory (GOBO). Our intention was to establish a hole that penetrates at least 100–200 m or as deep as possible into the basaltic basement. Although we did not intend to core sedimentary rocks, basement rocks were to be cored to allow a wide range of petrological, geochemical, and geophysical studies on the rock samples recovered. The extent of the coring and penetration into basement was to be much greater than previous drilling at either Sites 756 or 757 along the Ninetyeast Ridge, where only a few tens of meters of penetration were achieved into basaltic basement. In addition, the intention was to obtain a full suite of logs from the borehole to assess its geometry and other geophysical parameters that would allow selection of an optimal position for installing the seismometer. The permanent seismometer instrumentation will be installed after drilling at a later date by a submersible or a surface ship. Simply establishing this cased reentry hole was to require up to a week of ship time. In addition to drilling and casing operations, a series of seismic experiments involving the drillship, as well as the research vessel *Sonne,* were also planned while on site. These experiments included seismic while drilling (SWD), vertical seismic profile (VSP), and an offset seismic experiment (OSE), as well as the possible deployment of a broadband wide dynamic range seismometer in the borehole to test the deployment procedure and shock resistance of the instrument.

Background

The scientific community has recognized that global seismic observations will remain incomplete until instruments are deployed on the ocean floor. There is asymmetry in station coverage between oceans and continents, and more particularly between the Southern and Northern Hemispheres. The need for ocean-bottom observatories for geodetic, magnetic, and seismic studies is driven by the same factor: the lack of observations in large tracts of the world ocean where neither continents nor islands are available to place observatories. Some plates (e.g., the Newsweek and Juan de Fuca Plates and the Easter Microplate) have no islands on which observatories are typically stationed, and, thus, the geodetic measurements needed to evaluate absolute plate motion and plate deformation are not available. The problem of extrapolating the magnetic field to the core/mantle boundary is greatly exacerbated by holes in observation sites in the Indian Ocean and eastern Pacific Ocean. Images of the interior velocity heterogeneity of the Earth, in turn related to thermal and chemical convection, are aliased by the lack of control from seismic stations in the Indian and Pacific Oceans. Maps of holes from all three disciplines include many common sites. It is now possible to consider installing joint observatories to meet the needs of all these programs. During workshops addressing the issue of GOBO (IRIS/Hawaii, 1993, ION-ODP, Marseilles, 1995), it was recognized that the installation of a GOBO is now feasible from a technological point of view and represents a high priority for the next 10 yr.

The installation of ocean-bottom seismic stations, their maintenance, and the recovery of data on a timely and long-term basis represent a formidable technical challenge. However, different pilot experiments carried out by Japanese (Kanazawa et al., 1992; Suyehiro et al., 1992), French (Montagner et al., 1994a, 1994b, 1994c), and Ameri-

can groups (OSN1, Dziewonski et al., 1992; J. Orcutt, pers. comm., 1998) demonstrate that there are technical solutions to all the associated problems.

The technical goal of the French Pilot Experiment OFM/SISMOBS (Observatoire Fond de Mer [ocean-floor seismometer]) conducted in April and May 1992 was to show the feasibility of installing and recovering two sets of three-component broadband seismometers (one inside an ODP borehole and another inside an ocean-bottom seismometer [OBS] sphere in the vicinity of the hole). Secondary goals were to (1) obtain the seismic noise level in the broadband range 0.5–3600 s, (2) conduct a comparative study of broadband noise on the seafloor, downhole, and on a continent, and (3) determine the detection threshold of seismic events. A complete description of the experiment can be found in Montagner et al. (1994a), and a summary drawing is presented in Figure F2.

F2. Sketch of the OFM/SISMOBS experiment, p. 16.

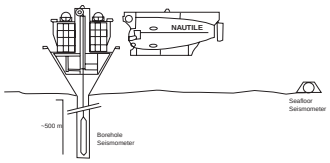

After the installation of both sets of seismometers, seismic signals were recorded continuously during 10 days. The analysis of these signals shows that the seismic noise is smaller in the period range 4–30 s for both an OBS and a borehole seismometer than in a typical broadband continental station such as spinning sidebands (SSBs). The noise is still smaller than the noise at SSBs up to 600 s for OBSs. The noise on vertical components is much smaller than on the horizontal ones. The difference might be explained by instrument settling. It was also observed that the noise level tends to decrease as time goes by for both ocean-bottom and borehole seismometers, which means that the equilibrium stage was not yet attained by the end of the experiment (Beauduin et al., 1996a, 1996b). The patterns of microseismic noise in oceanic and continental areas are completely different. The background microseismic noise is shifted toward shorter periods for ocean-bottom and borehole seismometers compared to a continental station. This might be related to the difference in the crustal structure between oceans and continents and to attenuation of seismic noise caused by ocean surface waves and currents. The low level of seismic noise implies that the detection threshold of earthquakes is very low, and it has been possible to correctly record teleseismic earthquakes of magnitude as small as 5.3 (Montagner et al., 1994b). It was also possible to extract the earth tide oceanic signal. Therefore, the experiment was a technical and scientific success and demonstrated that the installation of a permanent broadband seismic and geophysical observatory at the bottom of the seafloor as well as in a borehole is now possible and can provide the scientific community with high-quality seismic data.

Scientific Objectives

Primary Objective

The primary objective of the Ninetyeast Ridge Observatory (NERO) portion of Leg 179 was to prepare a seafloor borehole for future establishment of a GOBO. This objective included drilling a single hole as deep as possible into basement, as well as installing a reentry cone and casing beyond basement to prepare the NERO site as an ocean-bottom observatory. The GOBO will be installed at a later time by Montagner and others and will be part of the future network of seafloor observatories proposed in the ION program.

The scientific objectives that can be addressed with geophysical data from long-term ocean-bottom observatories include two broad subject

areas: Earth structures and natural hazards. These two areas can each be divided into subareas according to the scale under investigation: global, regional, and local:

1. Global scale: mantle dynamics, core studies, moment tensor inversion. The ION report emphasizes that "oceans are seismic deserts" (this also applies to geomagnetic observatories). Except for a few stations on oceanic islands, very large zones are unmonitored, particularly in the Pacific, South Atlantic, and east Indian Oceans. With the present station coverage (FDSN [Federation of Digital Seismic Networks], Fig. **F3**), the best expected lateral resolution is >1000 km. There are many shadows or poorly illuminated zones in the Earth. Because of the nonuniformity of earthquake and seismic station distribution, seismic waves recorded in stations do not illuminate the whole Earth. For example, the transition zone (in a broad sense: 400–1000 km of depth) is poorly covered by surface waves and body waves below oceanic areas.
2. Regional scale (wavelengths between 500 and 5000 km): oceanic upper mantle dynamics, lithosphere evolution, and tsunami warning and monitoring. In terms of oceanic upper mantle seismic investigations, only very long wavelengths have been investigated. In addition, surface waves are the only waves sampling the oceanic upper mantle, and there are no direct measurements of body waves. To understand the lithosphere's evolution, it is necessary to improve the lateral resolution of tomographic seismic studies. The Indian Ocean crust is considered to be the most complex in any ocean basin. Since the 1970s, magnetic anomalies, fracture zone information, and other geophysical information (McKenzie and Sclater, 1971; Norton and Sclater, 1979; Schlich, 1982; Royer and Sandwell, 1989) have been used to understand the tectonic history of the Indian Ocean, which is characterized by irregularities in kinematic behavior (e.g., ridge jumps, reorganization of the ridge system, asymmetric spreading, spreading velocity changes, and, finally, collision between India and Asia). Few tomographic investigations have been performed so far in the Indian Ocean (Montagner, 1986; Montagner and Jobert, 1988; Leveque and Debayle, 1995). These studies display a good correlation between surface tectonics and seismic velocities down to 100 km, but there seems to be some offset at deeper depths for the Central Indian Ridge as a consequence of the decoupling between the lithosphere and the underlying mantle. This complexity at deeper depths is also present in global tomographic models. However, the lateral resolution is still quite poor, and it makes it necessary to increase the station coverage of oceanic areas. The next step in tomographic techniques requires the simultaneous use of surface waves and body waves. By installing only one station in the central Indian Ocean, it will be possible to obtain direct measurements of delay times and, therefore, unique and fundamental information on the local anisotropy (from SKS splitting), particularly for the 410 and 660 km discontinuities (from converted seismic waves) and for pure oceanic paths. As shown in Figure **F4,** the future observatory is surrounded by seismically active areas. This ensures that there will be a reasonable amount of data within 1 or 2 yr after borehole instrumentation.

F3. Location of the FDSNs and GEOSCOPE stations in the world as of 1996, **p. 17.**

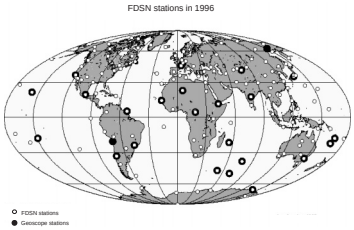

F4. Focal mechanisms of earthquakes that occurred in the Indian Ocean during the last 15 yr, **p. 18.**

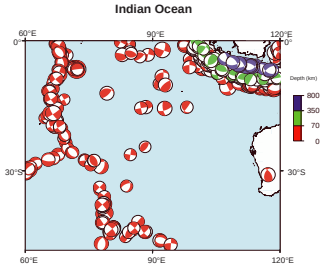

3. Local scale (wavelengths <500 km): oceanic crustal structure, sources of noise, and detailed earthquake source studies (tomography of the source, temporal variations).

Ancillary Objectives: SWD/VSP

One of the ancillary objectives of Leg 179 was to develop a SWD capability for ODP. The SWD project was funded by the National Science Foundation. SWD uses OBSs to listen to the drillship noise and does not use a VSP tool in the well. SWD has the potential for observing shear waves generated by the drill bit. Of the number of seismic experiments planned for Leg 179, SWD was the only experiment that did not use additional ship time, and it was the only experiment that could be kept in the operational schedule. This was because of contingencies (see below) that resulted in the limited time to achieve the primary objective of drilling the NERO hole.

VSPs have proven extremely useful over the history of ODP in correlating borehole properties with regional seismic properties. Normally they are carried out with a borehole seismometer and air gun shots fired on the surface from a second ship. Typically they take 6–12 hr of drillship time, depending on the depth of the hole, sampling interval, and so forth. In a SWD/VSP experiment, the seismic source is the drill bit, and the sound is received on geophones at the seafloor. SWD technology was developed for land boreholes using surface geophones and has had considerable success.

As a test effort, two OBSs and a drill-pipe pilot sensor were employed during Leg 179. OBSs were deployed and recovered at the NERO site, with initial results and procedures analyzed on board (see **"Seismic While Drilling,"** p. 10). The OBSs were deployed, and their locations were surveyed using the ship in dynamic positioning mode during pipe trips to and from the seafloor borehole.

Initial proof-of-concept of SWD consisted of three objectives:

1. A demonstration of the generation and recording of drill-bit signal on the pilot sensors at the rig floor. Analysis consists of producing filtered autocorrelation functions at depth intervals of <5 m over a range of bit depths sufficient to see pipe multiple arrivals and their characteristic moveout. Spectral and temporal characteristics of drill-bit signal will be documented.
2. A demonstration of the recording of drill-bit direct arrivals (*P*- and *S*-waves) in the OBS data. Analysis will consist of producing filtered cross-correlation functions (between the OBS and pilot sensor data) at depth intervals of <5 m over a range of bit depths sufficient to observe *P*- and *S*-wave moveout. Filtering will include polarization filtering, band-pass filtering, and multichannel spatial filtering so that direct arrival signals can be distinguished from other interference.
3. A demonstration of the recording of *P*- and *S*-reflections. Analysis will consist of waffled separation of direct and converted energy and isolation of primary bit-generated reflections.

The work necessary to establish a SWD capability fell into three categories: (1) acquisition of the OBS data during drilling, (2) acquisition of the pilot sensor data on the rig floor during the drilling operations, and (3) reduction of the OBS and pilot sensor data to a VSP format for seismic analysis. The work that belongs to the third category will mainly be done

postcruise because the data from the pilot sensor were not provided in digital form during Leg 179. The United States Geological Survey (USGS) OBSs used during Leg 179 both have three-component inertial sensors and hydrophones and can record autonomously on the seafloor for about 1 week. The pilot sensor data was acquired on the rig floor. Measurement while drilling technology (but not SWD) was tested during Leg 156 (Shipley, Ogawa, Blum, et al., 1995).

Modification of Objectives at Sea

Because of the delays caused in port at Cape Town, South Africa, delays in waiting for a resupply ship to arrive at Site 1105 on the Southwest Indian Ridge, and longer than expected transits, the operational schedule for NERO was severely impacted and had to be curtailed. The total number of days spent on site was reduced from 11.5 to 5.5, which resulted in barely enough time to meet the primary objective of drilling and casing the NERO hole for installation of the borehole seismometer. This was the highest remaining priority of Leg 179 and superseded all others. We were able to conduct the SWD experiment simply because it involved no additional ship time. In addition, components of the primary objective including coring basement, opening the borehole to depths of 200 m, and logging the hole had to be eliminated from the operational schedule. Ancillary objectives to the NERO hole also were not possible. These included the OSE experiment, the VSP experiment, and test deployment of the broadband seismometer.

Site Selection and Characteristics

Virtually all of the current "global" seismic network resides on land, creating large gaps in coverage for the ~71% of the Earth's surface below sea level. These gaps produce both bias and incomplete images of the Earth's interior. The ION project hopes to fill some of these major gaps in the Indian and Pacific Oceans by installing borehole seismometers in places that are at least 2000 km from any continent or ocean island where a possible seismic station observatory could be established. The site chosen for NERO fits this criteria.

Hole 1107A drilled during Leg 179 lies midway between Holes 757B and 757C, which are 200 m apart. These holes were drilled during Leg 121. Hole 1107A is located at 17°07.4180′S, 88°10.8497′E along the crestal portion of the Ninetyeast Ridge (Fig. **F1**). The hole was positioned to drill into the sedimentary cover and the underlying basaltic basement sampled during Leg 121 (Shipboard Scientific Party, 1989). The Ninetyeast Ridge is the product of a long-lived hot spot located near the Kerguelen archipelago, which is thought to have also formed the Broken Ridge, the Kerguelen-Heard Plateau, and the Rajmahal Traps in eastern India (Luyendyck and Rennick, 1977; Duncan, 1981, 1991; Saunders et al., 1991; see Fig. **F5**). The basaltic basement at the proposed site along the Ninetyeast Ridge includes eruptive units thought to have formed above a mantle plume in the southern Indian Ocean (e.g., Duncan, 1991; Saunders et al., 1991).

Previous drilling (Shipboard Scientific Party, 1989) at Holes 757B and 757C penetrated 369-m-thick sedimentary sequence that consisted from top to bottom of Eocene–Pleistocene nannofossil ooze, lower Eocene calcareous ooze and chalk, followed by ash, tuff, lapilli, and pebbly material. Below the sediment cover, Hole 757C penetrated 42 m of basaltic basement dated at 58 Ma by Duncan (1991). Site 1107 was

F5. Free-air gravity image derived from satellite altimetry of the Ninetyeast Ridge, Kerguelen Plateau, and Broken Ridge, **p. 19.**

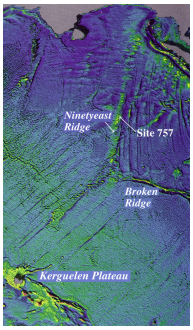

selected in close proximity because of the generally good drilling conditions and penetration rates experienced during Leg 121. Holes 757B and 757C were drilled at water depths of 1652.1 and 1643.6 m, respectively. Hole 1107A was drilled at a water depth of 1648 m. Drilling was expected to encounter roughly 370 m of sedimentary cover above basement, based on Leg 121 results.

One inherent problem in ocean borehole seismic observatories is the noise levels created at the sea surface, which is derived from wind and waves through direct forcing at long periods and by nonlinear coupling of elastic waves at short periods (Webb, 1998). Based on experience in Hole OSN-1, in which a borehole seismometer has already been deployed south of Hawaii, fairly high seismic noise levels were problematic (Dziewonski et al., 1992). The problem has been attributed to two factors. One is that the borehole casing is thought to have penetrated only 9 m into basement, and the seismic sonde was clamped to the casing. It is thought that the sonde was clamped above the basement/sediment interface (J. Orcutt, pers. comm., 1998). This problem was accommodated in the planning of Hole 1107A by casing to at least 40 m into basement. In a related problem, others have suggested that the noise level is high because the noise is coupled into the top of the borehole at the massive exposed reentry cone and propagates down a poorly cemented casing (Webb, 1998). In this case, proximity of the seismic sonde to the casing may also be problematic, so assuring a good cemented bond for the casing and/or deepening the hole significant distances below the casing should improve the noise level. In this way, the seismic sonde can be either clamped to the borehole wall or grouted into the borehole at a significant distance away from the casing (Webb, 1998; J. Orcutt, pers. comm., 1998). Others have suggested filling the borehole with sand. In the case of Hole 1107A, our drilling strategy included deepening the borehole beyond the casing as much as time allowed. At least 10 m was required for the installation of the seismometer. Our drilling plan involved washing through the sedimentary cover to 370 m and then drilling 40 m into basement. The borehole would then be cased and cemented, and, finally, the borehole would be cored and drilled to a maximum depth of 200 m below the sediment/basement interface. Because of the time problem described above, we developed a no-coring strategy to maximize penetration through the cement and into the borehole with the small time available. The strategy fell short of saving enough time for the OSE experiment, but it allowed us to drill through the casing shoe, cement, and rathole fast enough to allow establishment and further deepening of the borehole.

OPERATIONS

Transit to Site 1107

The 1930-nmi transit from Site 1106 to Site 1107 was accomplished in 7.8 days at an average speed of 10.2 kt. During the transit, preparations were made for deploying a reentry cone and casing. The reentry cone was assembled and moved onto the moonpool doors. The 16-in casing string was strapped, and a casing shoe was installed on the end of the 16-in shoe joint. The 16-in casing string was laid out on top of the riser hatch for immediate deployment upon arrival. The 10¾-in casing string was strapped and rabbeted in the riser hold, where it remained until time for deployment. The 16- and 10¾-in casing hang-

ers and running tools were moved to the rig floor and fit tested. The 10¾-in cementing equipment, including the cementing head, kelly cock valve, and subsea release (SSR) plug, were also moved to the rig floor. The vessel arrived in the immediate area of the proposed site at 2012 hr on 22 May to be greeted by the *Sonne*. A positioning beacon was deployed at 2024 hr on 22 May, on the Global Positional System coordinates for the proposed site, officially establishing Site 1107.

Hole 1107A

The reentry cone was positioned in the center of the moonpool doors. The 48.8-m 16-in casing string was made up and latched into the reentry cone in ~5 hr. Making up the 16-in casing was slowed by excessive roll caused by two large cross swells affecting vessel stability. The jetting bottom-hole assembly (BHA) was made up of a 14¾-in bit, a bit sub, five 8¼-in drill collars, a 16-in Dril-Quip CADA casing running tool, two 8¼-in drill collars, a tapered drill collar, and two stands of 5½-in drill pipe. The jetting BHA was latched into the 16-in casing hanger, and the reentry cone/16-in casing string assembly was lowered to the seafloor. The camera was also deployed to observe the position of the reentry cone after jetting in and to observe release of the 16-in casing running tool.

No pilot hole or jet test was performed before jetting in the 16-in casing at Hole 1107A. The location of Hole 1107A was positioned between Holes 757B and 757C, which are 200 m apart and were drilled during Leg 121. The length of 16-in casing to be jetted in at Hole 1107A was determined based on advanced hydraulic piston corer data from Leg 121. Also, the seafloor depth established during Leg 121 was used for starting the jetting in process for Hole 1107A. However, the official water depth of 1659 mbrf was determined by tagging the seafloor with the end of the 16-in casing, which was determined to occur at the first noticeable pressure change while initiating the jetting in process.

Jetting in of the 16-in casing began at 1455 hr on 23 May, establishing Hole 1107A. Jetting in the 48.8-m of 16-in casing was accomplished in 2 hr, 21 min. The camera was used to determine that the reentry cone mud mat was positioned properly, sitting on the seafloor. The 16-in casing running tool was unlatched and retrieved with no difficulties. During the trip out of the hole, two Woods Hole Oceanographic Institution (WHOI) OBSs were deployed and surveyed relative to Hole 1107A as part of a SWD experiment. A ship-to-ship transfer from the *Sonne* of blasting caps and a ranging transducer was also completed.

Once back on deck, the 16-in casing running tool was removed and an additional 8¼-in drill collar was added to make up the 14¾-in drilling BHA. The 14¾-in drilling BHA was tripped to the seafloor, and the reentry cone reentered at 0543 hr on 24 May. The hole was drilled ahead to a depth of 2081 mbrf (422 mbsf) with mud sweeps as follows: 1 × 25 bbl at 1810.4 mbrf (151.4 mbsf); 1 × 25 bbl at 1897 mbrf (238.1 mbsf); and 1 × 30 bbl at 2081 mbrf (422 mbsf). As soon as the BHA was below the seafloor the Lamont-Doherty Earth Observatory (LDEO) sensor sub, part of the SWD experiment, was installed. The sediment portion of the hole drilled slower than anticipated with rates of penetration (ROPs) as low as 4 m/hr. However, the hole remained stable with little, if any, fill at connections.

Contact with basement was made at a depth of ~2030 mbrf (371 mbsf). Unlike the sediments, the basement initially drilled faster than anticipated with ROPs as high as 8 m/hr. The original drilling plan

called for ending the 14¾-in hole at a depth of 2069 mbrf (410 mbsf). However, firm basement was not encountered until a depth of 2063 mbrf (404 mbsf) had been reached. Therefore, the decision was made to continue drilling ahead until at least one full joint of casing could be positioned below the hard basement contact.

A wiper trip was made to a depth of 1692 mbrf (33 mbsf, inside the 16-in casing) with a maximum overpull of 10,000 lb. The LDEO sensor sub was removed during the wiper trip in preparation of running the 10¾-in casing string. The hole was allowed to stabilize for 1 hr, and then the bit was slowly tripped back to bottom. A moderate drag of 20,000 lb was observed near the sediment/basement contact at a depth of 2035 mbrf (376 mbsf). The top drive was picked up, and the hole was washed and reamed through the sediment/basement contact area. Once the bit was back on bottom, the hole was swept with a 30-bbl mud pill and then displaced with 346 bbl of sepiolite mud. The bit was then retrieved in preparation for deploying the 10¾-in casing string.

A 413.2-m-long string of 10¾-in casing, including the remaining 23 joints of 10¾-in standard coupling casing on board, was made up in ~5 hr. A cementing BHA consisting of a 10¾-in SSR cementing plug, a 10¾-in Dril-Quip casing running tool, five 8¼-in drill collars, a tapered drill collar, and two stands of 5½-in drill pipe was made up and latched into the 10¾-in casing string. The 10¾-in casing string was then tripped to the seafloor, and Hole 1107A was reentered at 1515 hr 26 May.

The casing was run to depth when the top drive, kelly cock valve (used to prevent cement from flowing up into the top drive), and cementing head were picked up. The drill string was then spaced out to land the 10¾-in casing hanger inside the 16-in casing hanger. After landing the 10¾-in casing hanger, latch-in was confirmed with a 10,000-lb overpull. From reentry to latch-in, confirmation took ~2 hr, with no difficulties encountered.

The 10¾-in casing was successfully cemented in place with 238 sacks (48.8 bbl) of silica flour blended 15.8 lb/gal cement. While displacing the cement, the pipe wiper plug dart was dropped on top of the cement slug and chased with a 10-bbl freshwater spacer and then seawater. Landing of the pipe wiper plug dart in the SSR plug was confirmed with an increase in drill-string pressure. While we pressured up the drill string to release the SSR plug, the cementing hose burst near the connection with the cementing head at ~2000 psi, requiring the pump to be shut down immediately. Fortunately, at that time the cement slug was contained within the casing below the SSR plug (with the latched in dart) and the casing shoe.

Using a tugger, the driller was raised in the derrick to the heaving cementing head, where he broke off the ruptured cementing hose and replaced it with a blanking plug. Once this was accomplished, the driller also had to manually open the kelly cock valve above the cementing head, so a circulation path through the top drive could be established. After the driller was safely back on the rig floor, the pump was re-engaged and the drill string pressured up immediately, indicating that the SSR plug and dart had remained in place. The drill-string pressure was increased to ~2800 psi when the SSR plug released and was pumped to the casing shoe. Upon landing of the SSR plug in the casing shoe, a solid 600-psi pressure was held for a few minutes. The stand pipe bleed-off valve was then opened, and no flow back was observed, indicating that the casing shoe valve was holding. The only task remaining was to release the casing running tool. It required ~45 min of

working the 10¾-in casing running tool before it finally was released and the drill string could be retrieved.

The original drilling plan called for coring Hole 1107A to a depth of ~200 into basement. However, with the lost time in port rebuilding the lower guide horn, there was not time to core at all, let alone hope to reach a depth of 200 m into basement. The decision was made to deploy a 9⅞-in tricone drill bit and drill as deep into basement as the remaining operational time allowed in the hope of leaving an acceptable hole for the future installation of an ION seismometer. A 9⅞-in drilling BHA was made up consisting of a 9⅞-in tricone bit, a bit sub, eight 8¼-in drill collars, a tapered drill collar, and two stands of 5½-in drill pipe. The 9⅞-in drilling BHA was tripped to the seafloor, and Hole 1107A was reentered at 0738 hr 27 May.

The 10¾-in casing shoe was drilled out in 43 min. The rathole below the 10¾-in casing shoe was cleaned out, and then a 9⅞-in-diameter hole was drilled into basement to a total depth (TD) of 2152.8 mbrf (493.8 mbsf, 122.8 m into basement, 79.4 m below the 10¾-in casing shoe, Fig. **F6**). A schematic drawing of the NERO borehole installation is shown in Figure **F6**. A single 25-bbl mud sweep was pumped at 2107.4 mbrf (448.4 mbsf). At TD the hole was flushed clean and a 30-bbl mud sweep was circulated. With the hole cleaned up as much as possible, and with operations time expiring, the bit was retrieved. The bit cleared the rotary table at 0640 hr 28 May, ending Hole 1107A. During the trip out of the hole, the two WHOI OBSs were recovered. The vessel was secured for sea and the transit to Darwin, Australia, began at 0730 hr on 28 May.

F6. Schematic illustration of the cased borehole configuration at Hole 1107A, **p. 20.**

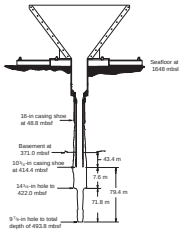

SEISMIC WHILE DRILLING

SWD Experiments at Site 1107

While drilling at Hole 1107A, measurements of the accelerations of the drill string and of ground- and water-borne seismic energy were made over a 31-hr interval beginning at 0400 on 24 May and concluding at 1109 on 25 May. The hole was jetted or drilled with a tricone roller bit (no cores) through 373 m of sediments. Drilling rates averaged 30 m/hr for the first 228 m and then slowed to an average of 24 m/hr for the lower sedimentary section. Basement was encountered at 373 m, and drilling rates to the initial target depth of 422 m were 3 to 4 m/hr. Concurrent drill-string accelerometer and two OBS measurements were made over the depth range 170 to 422 m. OBS measurements were also made in drilling from 48 to 170 m and, after setting casing, from 422 to 493 m.

The two OBSs were deployed at ~1330 on 23 May and recovered at ~2000 on 27 May. The data from each OBS were recorded in one continuous (500 and 674 MB) file (200 samples/s, two bytes/sample, three or four channels) for 4 days. The proximal OBS (#A8) recorded three channels consisting of a vertical geophone and two horizontal geophones. The distal one (#A4) recorded a vertical and two horizontal components and a hydrophone. The accelerometer data (400 samples/s, two bytes/sample, three channels, and 1-s headers) are in 30-min (4.464 MB) files, totaling 277 MB for the 31 hr.

The OBS data concurrent with the accelerometer data were extracted from the two complete OBS data files and converted into 40-s traces (SEGY format) for plotting and correlation purposes. The trace length

was arbitrarily chosen. This produced working files consisting of 5598 traces out of the 9224 recorded.

Figure F7 compares samples of drill-string acceleration spectra during drilling in the lower sediment section at 225 m and in basement at 375 m. The principal spectral component at 2.5 Hz appears to be the drill-string rotation rate (51 rpm) times the number of roller cones (three). Similarly in the lower plot, the 3.4-Hz component appears to be the drill-string rotation rate (67 rpm) times the number of roller cones (three). The cutting action of the bit in hard rock produces more sound energy, much of it in the frequency range of 32 to 50 Hz.

In the 30-s sample of drilling in basement shown in Figure F8, the coherence between comparable channels on the two OBS recordings is not as high as anticipated. The spectrum shows considerable energy in the interval 10 to 40 Hz, indicating that hard-rock drilling produces more and higher frequency energy than the sediment drilling. It was not possible to perform a more detailed study regarding the correlation of OBS and drill-string accelerometer data on board because the accelerometer recordings were not provided in digital form during the leg.

F7. Amplitude spectra of drill-string accelerometer, p. 21.

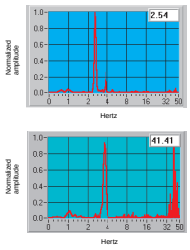

F8. A 30 s sample of the time series and spectra during drilling in basement at 398 m, p. 22.

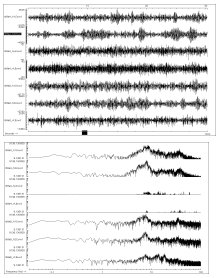

Two-Ship Seismic Experiment at Site 1107

During the *Resolution's* stay at Site 1107, the German research vessel *Sonne* was conducting a geophysical survey of the area (Flueh and Reichert, 1998) using 25 ocean-bottom hydrophones and ocean-bottom seismometers. Data files containing shot positions and times of four profiles that were shot by the *Sonne* while the two OBSs were deployed from the *Resolution* were transmitted from the *Sonne* to the *Resolution* via e-mail.

Based on the shot information (shot positions are shown in Fig. F9; Table T1), OBS data was converted to SEGY-format, 20-s traces with an 8 km/s reduction velocity, and added to the GEOMAR dataset. Figure F10 shows the data for the Profile P8, which passed close by. The noise level of these data is somewhat greater because of the proximity and sound level of the *JOIDES Resolution*. Crustal *P*- and *S*- arrivals are clearly shown, but no refracted or reflected arrivals from the mantle are recorded because of the short length of the profile. The curvature of the crustal phases indicates high-velocity gradients. The different components of the OBS recordings are revealing some information on the nature of the seismic phases (Fig. F10). The amplitude of the *P*-wave first arrivals is strong on the hydrophone and the vertical geophone and is very weak on the horizontal geophones. The hydrophones show strong water multiples, whereas the horizontal geophones have strong pegleg multiples (arrivals that bounce within the sedimentary layer). The pegleg multiples may be better detected by the horizontal channels because their angle of emergence is low. The vertical component of OBS #A4 has a poor signal-to-noise ratio compared to the other recordings, probably because low frequencies are filtered out by the instrument (see also Figs. F85, p. 163; F86, p. 164; both in the "Hammer Drill Site" chapter). For a further interpretation, these data have to be included in the GEOMAR dataset.

Additional two-ship work had been planned (see "Vertical Seismic Profile," p. 17, in the Explanatory Notes chapter), but time did not allow execution.

F9. Location of some of the *Sonne* seismic reflection/refraction profiles in the vicinity of Site 1107, p. 23.

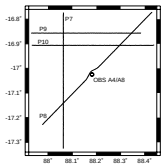

T1. Profiles shot by the *Sonne* during OBS deployment, p. 28.

F10. Travel-time/distance plots for profile P8 for each of the components recorded by OBSs #A4 and #A8, p. 24.

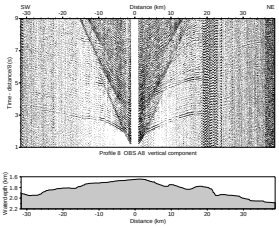

Locating the OBSs on the Seafloor

At the third deployment in 1660 m water depth, OBS #A4 was dropped at 300 m east of the hole and landed at 210 m 116° from the hole. OBS #A8 was dropped at 100 m east of the hole and landed at 81 m 165° from the hole. In both cases, this was southwest of the drop locations. Drifts were 6.5% and 5.8% of the water depth, respectively. The surveying procedure was the same as at Site 1105. The estimate precision is 30 m.

REFERENCES

Beauduin, R., Lognonn, P., Montagner, J.-P., Karczewski, J.F., and Morand, M., 1996a. The effects of atmospheric pressure changes on seismometers: a matter of installation. *Bull. Seis. Soc. Am.,* 86:760–1769.

Beauduin, R., Montagner, J.-P., and Karczewski, J.-F., 1996b. Time evolution of broadband seismic noise during the French experiment OFM/SISMOBS. *Geophys. Res. Lett.,* 23:2995–2998.

Duncan, R.A., 1981. Hotspots in the southern oceans: an absolute frame of reference for motion of the Gondwana continents. *In* Solomon, S.C., Van der Voo, R., and Chinnery, M.A. (Eds.), *Quantitative methods of assessing plate motions*. Tectonophysics, 74:29–42.

Duncan, R.A., 1991. Age distribution of volcanism along aseismic ridges in the eastern Indian Ocean. *In* Weissel, J., Peirce, J., Taylor, E., Alt, J., et al., *Proc. ODP, Sci. Results,* 121: College Station, TX (Ocean Drilling Program), 507–517.

Dziewonski, A., Wilkens, R., Firth, J. and Shipboard Scientific Party, 1992. Background and objectives of the Ocean Seismographic Network and Leg 136 drilling results. *In* Dziewonski, A., Wilkens, R., Firth, J., et al., *Proc. ODP, Init. Repts,* 136: College Station, TX (Ocean Drilling Program), 3–8.

Flueh, E.R., and Reichert, C., 1998. Cruise Report SO 131 SINUS. GEOMAR Rep. 72:337.

Kanazawa, T., Suyehiro, K., Hirata, N., and Shinohara, M., 1992. Performance of the ocean broadband downhole seismometer at Site 794. *In* Tamaki, K., Suyehiro, K., Allan, J., McWilliams, M., et al., *Proc. ODP, Sci. Results,* 127/128 (Pt. 2): College Station, TX (Ocean Drilling Program), 1157–1171.

Leveque, J.J., and Debayle, E., 1995. Anisotropic structure of the upper mantle in the Indian Ocean by waveform inversion. *IUGG,* 21:375. (Abstract)

Luyendyk, B.P., and Rennick, W., 1977. Tectonic history of aseismic ridges in the eastern Indian Ocean. *Geol. Soc. Am. Bull.,* 88:1347–1356.

McKenzie, D., and Sclater, J.G., 1971. The evolution of the Indian Ocean since the Late Cretaceous. *Geophys. J. R. Astron. Soc.,* 24:437–528.

Montagner, J.-P., 1986. Three-dimensional structure of the Indian Ocean inferred from long-period surface waves. *Geophys. Res. Lett.,* 13:315–318.

Montagner, J.-P., and Jobert, N., 1988. Vectorial tomography: II, application to the Indian Ocean. *Geophys. J. R. Astron. Soc.,* 94:309–344.

Montagner, J.P., Karczewski, J.F., and Romanowicz, B., 1994a. A first step toward an oceanic geophysical observatory. *Eos,* 75:150–154.

Montagner, J.P., Karczewski, J.F., Floury, L., and Tarits, P., 1994b. Towards a geophysical ocean bottom observatory. *Seismic Waves,* 3:7–9.

Montagner, J.P., Karczewski, J.F., Romanowicz, B., Bouaricha, S., Lognonne, P., Roult, G., Stutzmann, E., Thirot, J.L., Brion, J., Dole, B., Fouassier, D., Koenig, J.C., Savary, J., Floury, L., Dupond, J., Echardour, A., Floc'h, H., 1994c. The French pilot experiment OFM-SISMOBS: first scientific results on noise level and event detection. *Phys. Earth Planet. Int.,* 84:321–336.

Norton, I.O., and Sclater, J.G., 1979. A model for the evolution of the Indian Ocean and the breakup of Gondwanaland. *J. Geophys. Res.,* 84:6803–6830.

Peirce, J., Weissel, J., et al., 1989. *Proc. ODP, Init. Repts.,* 121: College Station, TX (Ocean Drilling Program).

Royer, J.-Y., and Sandwell, D.T., 1989. Evolution of the eastern Indian Ocean since the Late Cretaceous: constraints from GEOSAT altimetry. *J. Geophys. Res.,* 94:13755–13782.

Saunders, A.D., Storey, M., Gibson, I.L., Leat, P., Hergt, J., and Thompson, R.N., 1991. Chemical and isotopic constraints on the origin of basalts from Ninetyeast Ridge, Indian Ocean: results from DSDP Legs 22 and 26 and ODP Leg 121. *In* Weissel, J.,

Peirce, J., Taylor, E., Alt, J. et al., *Proc. ODP, Sci. Results,* 121: College Station, TX (Ocean Drilling Program), 559–590.

Schlich, R., 1982. The Indian Ocean: aseismic ridges, spreading centers, and oceanic basins. *In* Nairn, A.E.M., and Stehli, F.G. (Eds.), *The Ocean Basins and Margins* (Vol. 6): New York (Plenum), 51–147.

Shipboard Scientific Party, 1989. Site 757. *In* Peirce, J., Weissel, J., et al., *Proc. ODP, Init. Repts.,* 121: College Station, TX (Ocean Drilling Program), 305–358.

Shipley, T.H., Ogawa, Y., Blum, P., et al., 1995. *Proc. ODP, Init. Repts.,* 156: College Station, TX (Ocean Drilling Program).

Suyehiro, K., Kanazawa, T., Hirata, N., Shinohara, M., and Kinoshita, H., 1992. Broadband downhole digital seismometer experiment at Site 794: a technical paper. *In* Tamaki, K., Suyehiro, K., Allan, J., McWilliams, M., et al., *Proc. ODP, Sci. Results,* 127/128 (Pt. 2): College Station, TX (Ocean Drilling Program), 1061–1073.

Webb, S.C. 1998. Broadband seismology and noise under the ocean. *Rev. Geophys.,* 36:105–142.

Figure F1. Site map in the eastern Indian Ocean showing the location of Ninetyeast Ridge, the NERO Site 1107, and other ODP/DSDP sites in the region. Contour is 3000 mbsl (from Peirce, Weissel, et al., 1989).

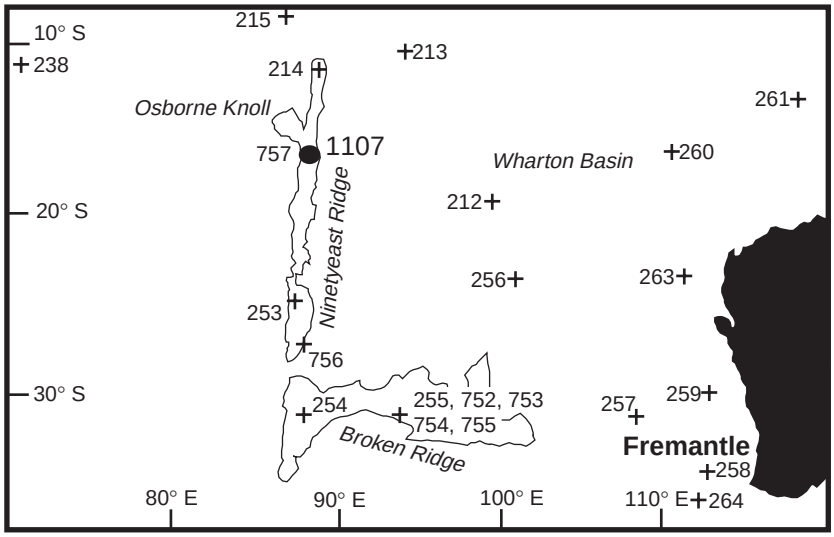

Figure F2. Sketch of the OFM/SISMOBS experiment (April–May 1992) (Modified from Montagner et al., 1994a).

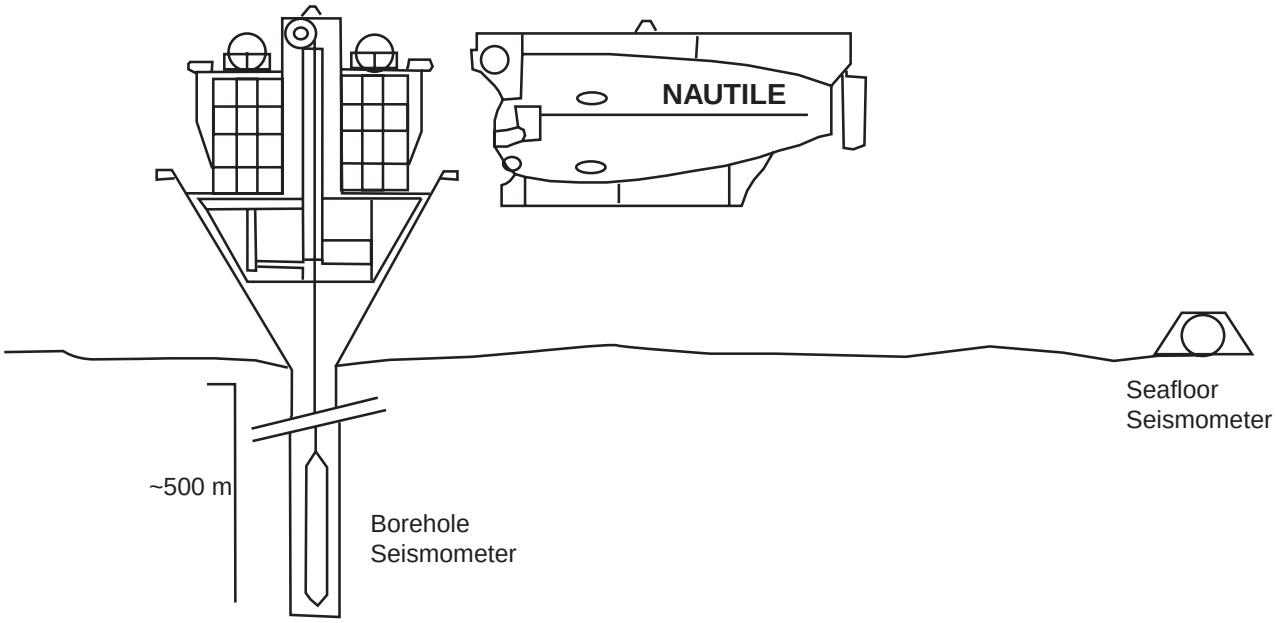

Figure F3. Location of the Federation of Digital Seismic Networks (FDSNs) and GEOSCOPE stations in the world as of 1996.

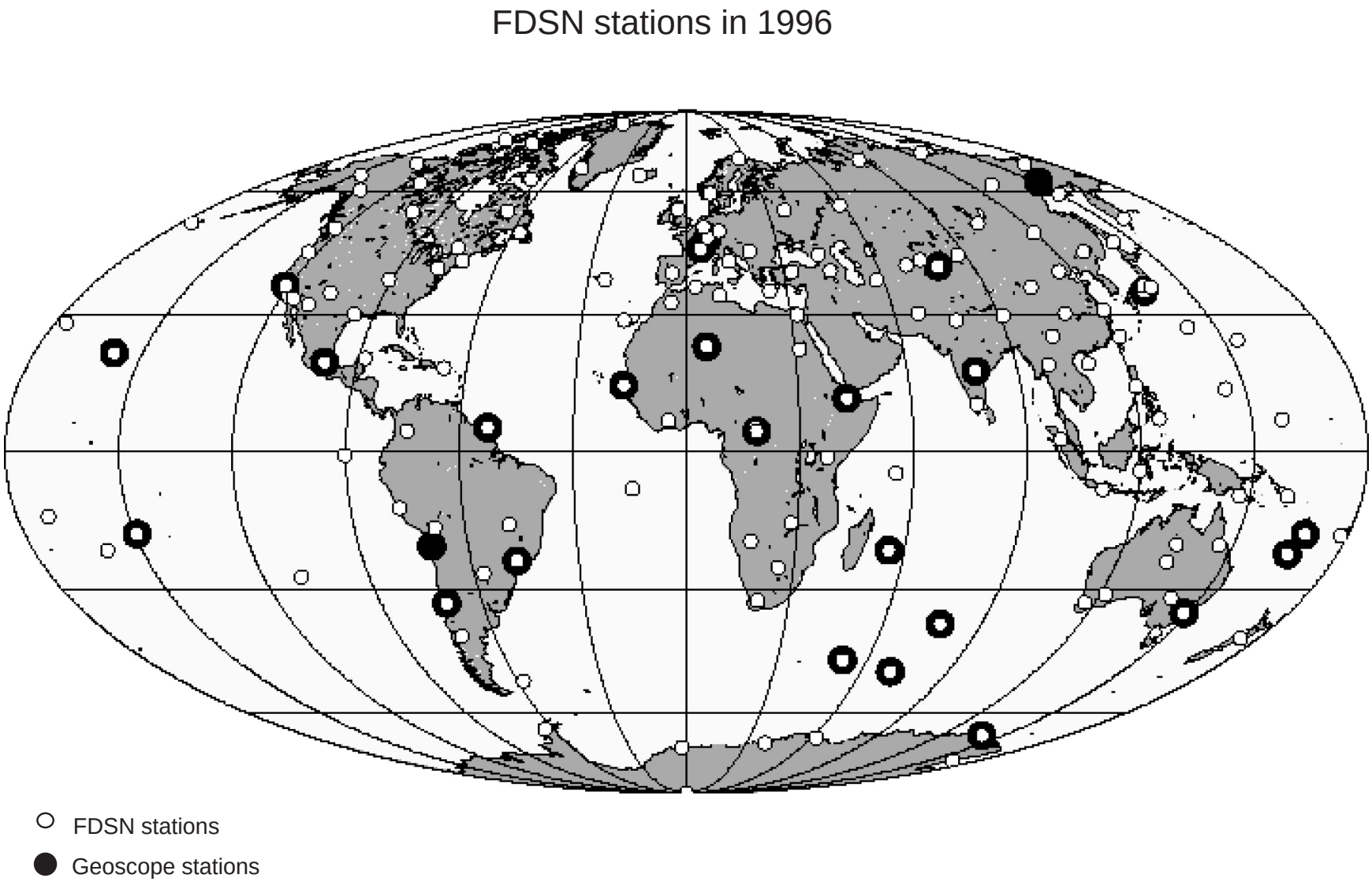

Figure F4. Focal mechanisms of earthquakes that occurred in the Indian Ocean during the last 15 yr (from the Harvard database). Beachball symbols are a graphic representation of earthquake source geometry/radiation pattern. Note that the Australo-Indian plate is characterized by a high intraplate seismicity.

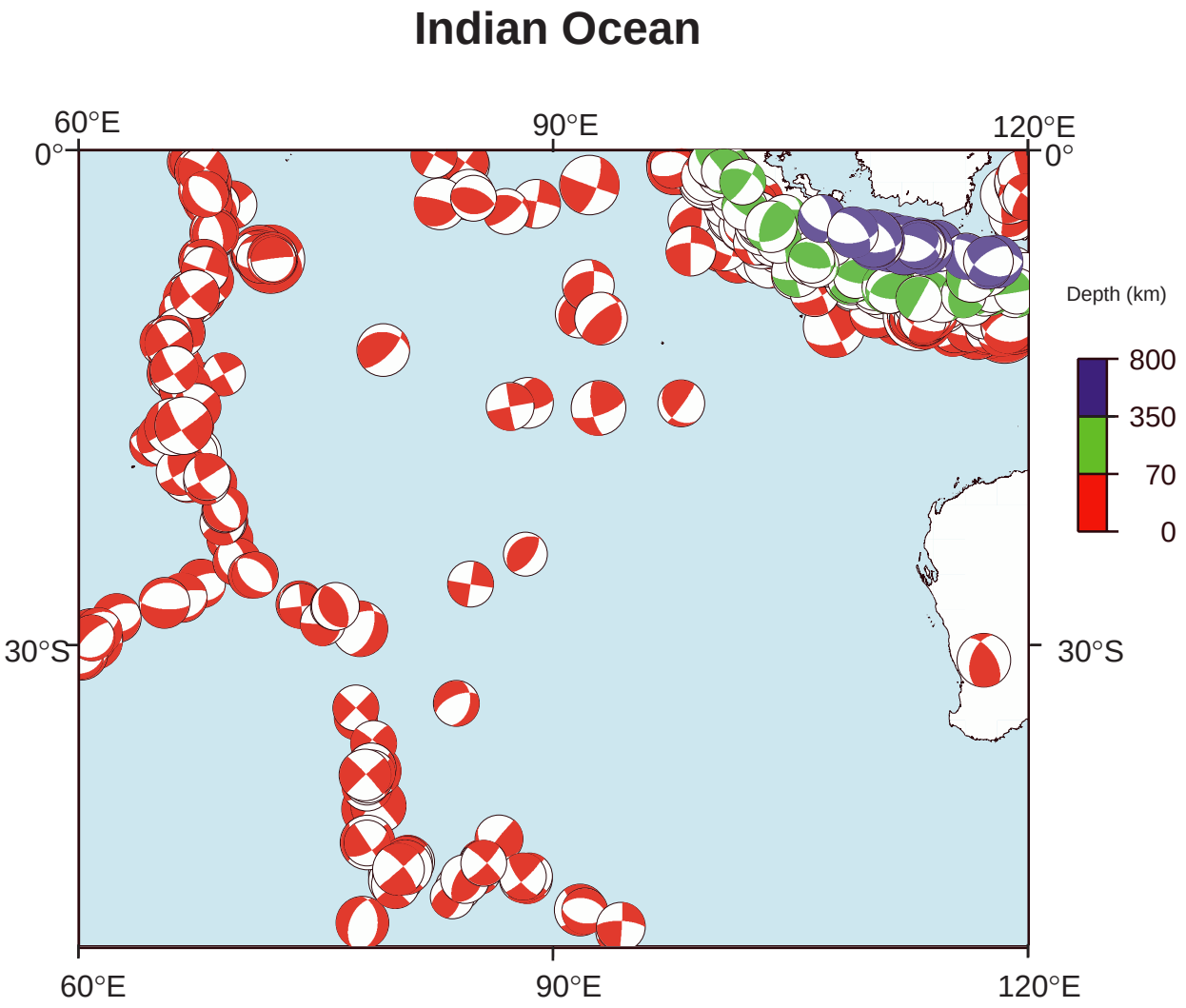

Figure F5. Free-air gravity image derived from satellite altimetry of the Ninetyeast Ridge and companion Kerguelen Plateau and Broken Ridge, all products of a long-lived hot spot located near the Kerguelen archipelago (e.g., Duncan, 1991).

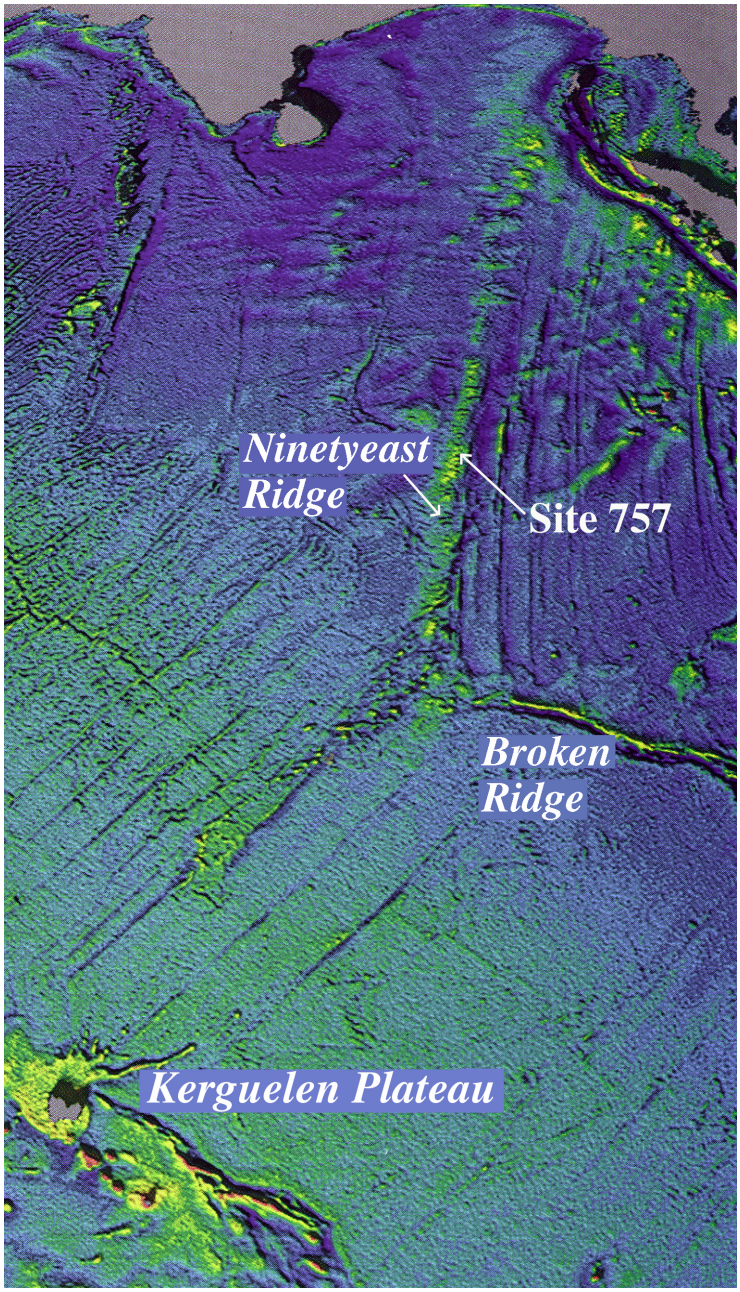

Figure F6. Schematic illustration of the cased borehole configuration at Hole 1107A.

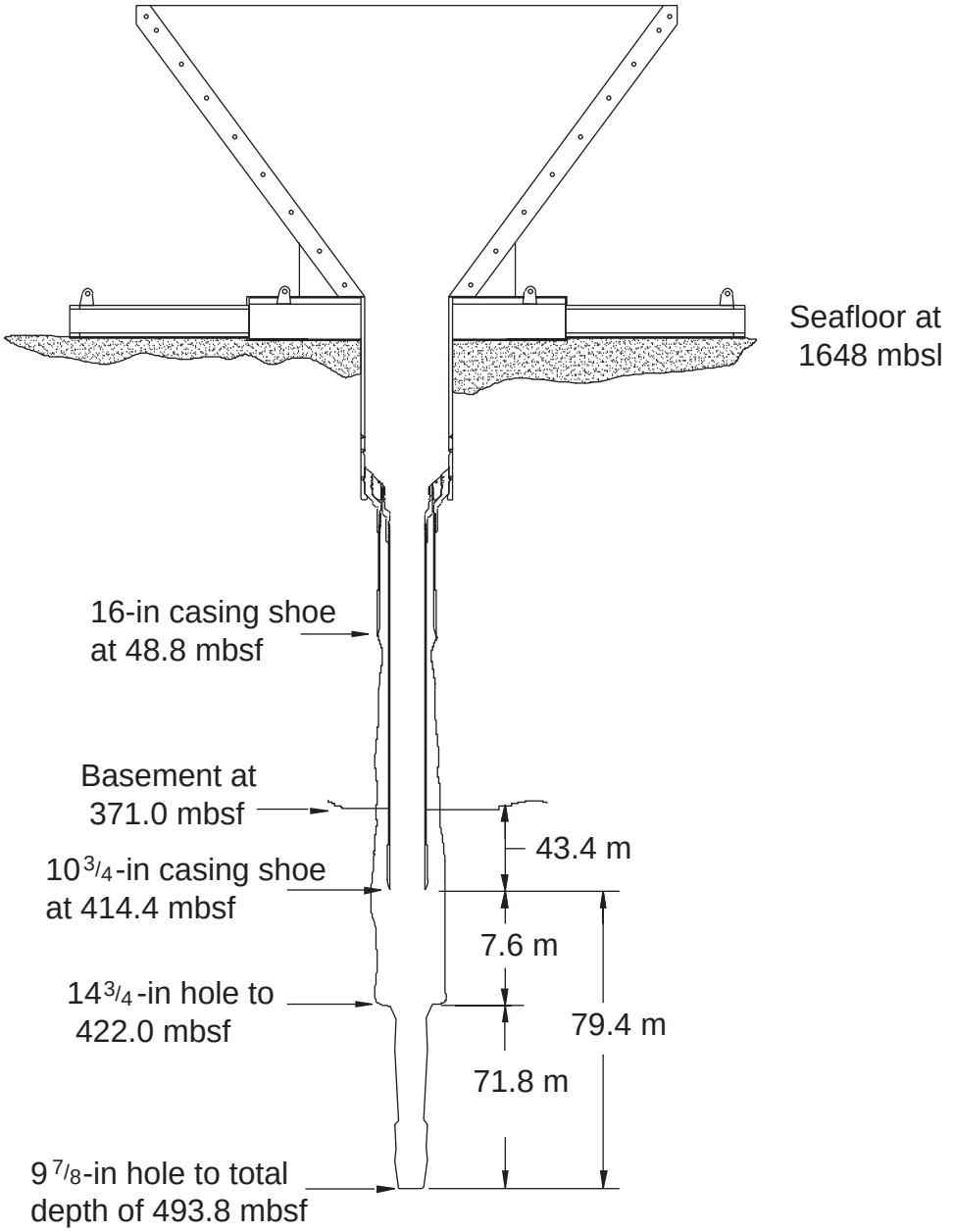

Figure F7. Amplitude spectra of the drill-string accelerometer. The upper trace is while drilling at 225 m in the upper sediment section; the lower is at 375 m in basement. The value of the greatest spectral component is shown in the upper right.

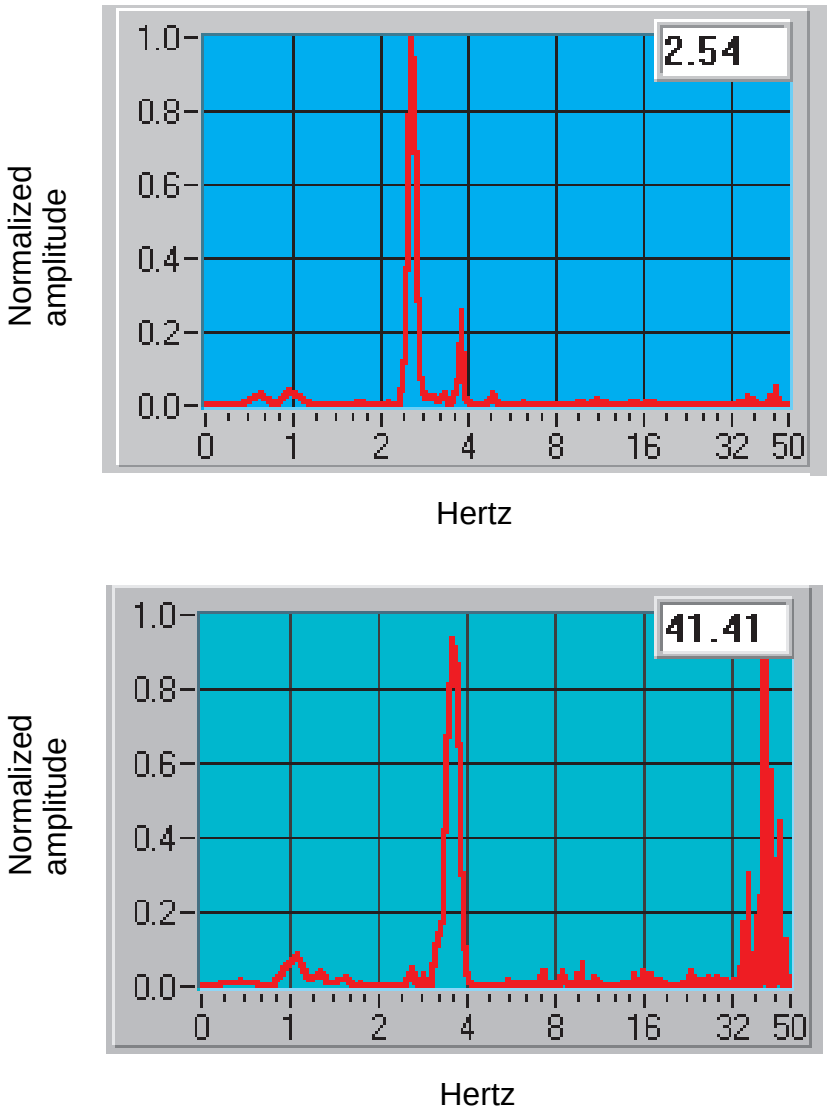

Figure F8. A 30-s sample of the time series (upper) and spectra (lower) during drilling in basement at 398 m. In each case, the lower three traces are the nearer seismometer, and the upper four the far seismometer. Note the differing amplitude scales for each trace.

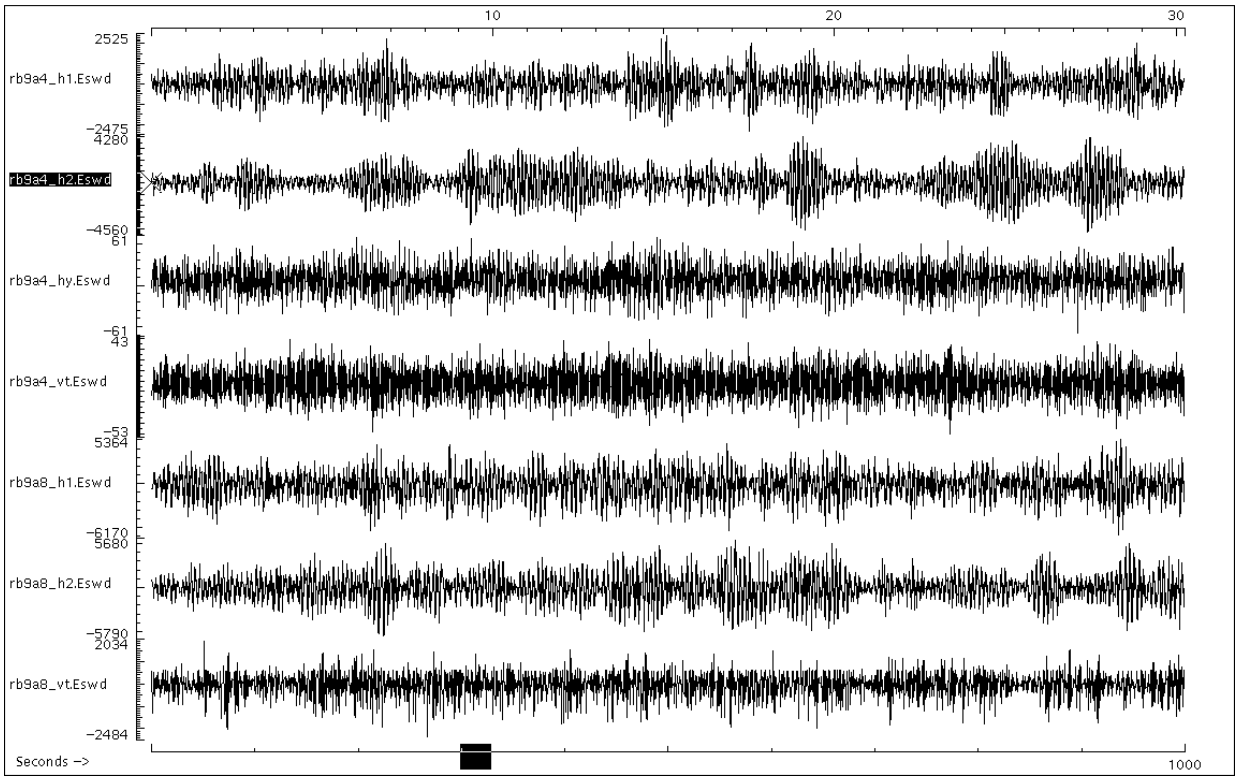

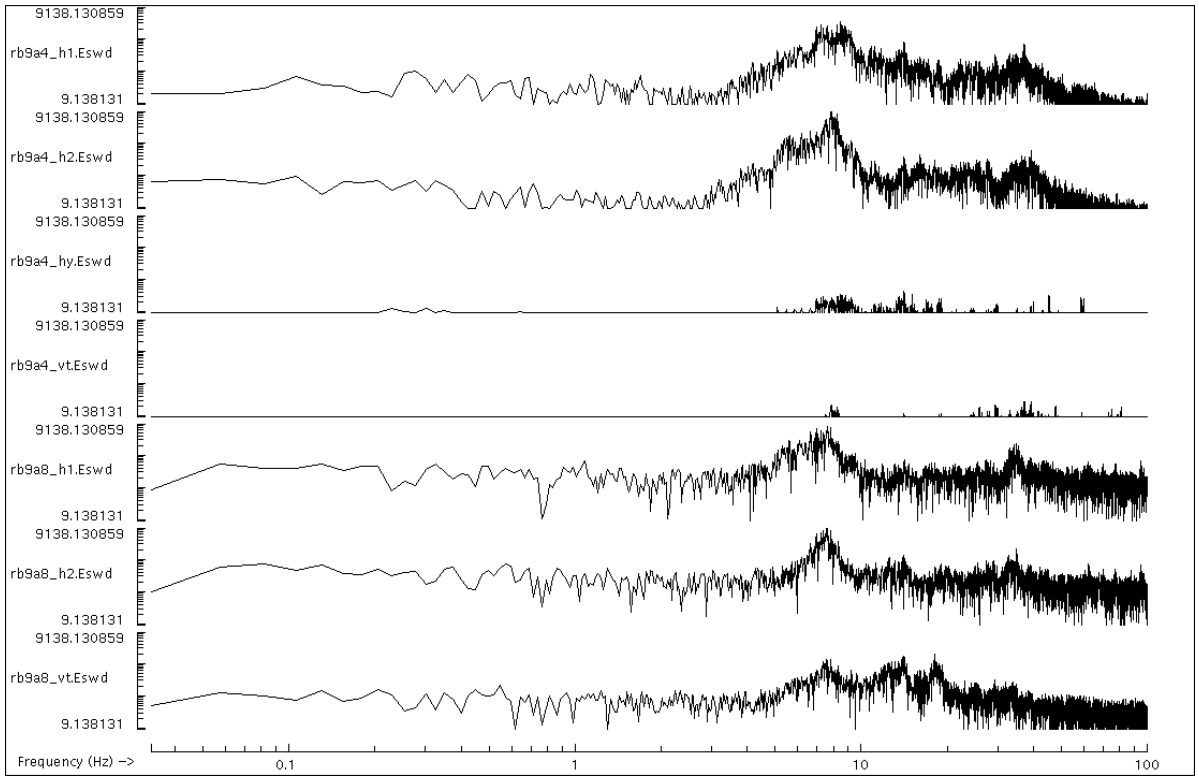

Figure F9. Location of some of the *Sonne* seismic reflection/refraction profiles in the vicinity of Site 1107. Air gun shots along these profiles were made by the *Sonne* during the recording time of OBSs #A4 and #A8.

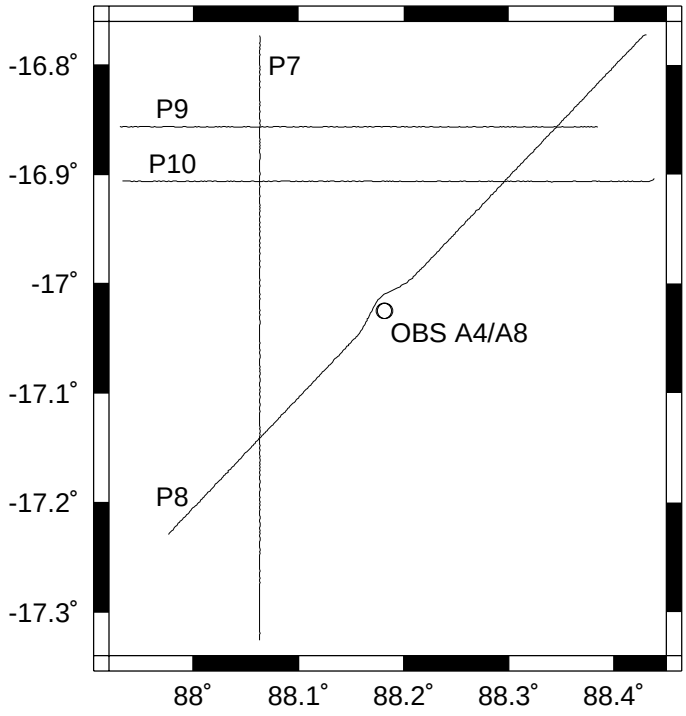

Figure F10. Travel-time/distance plots for each of the components recorded by OBSs #A4 and #A8 during shooting of profile P8. The data are band-pass filtered from 2/6 to 16/24 Hz, and the level plotted is proportional to offset. The seafloor topography is shown at the bottom. (Continued on next three pages.)

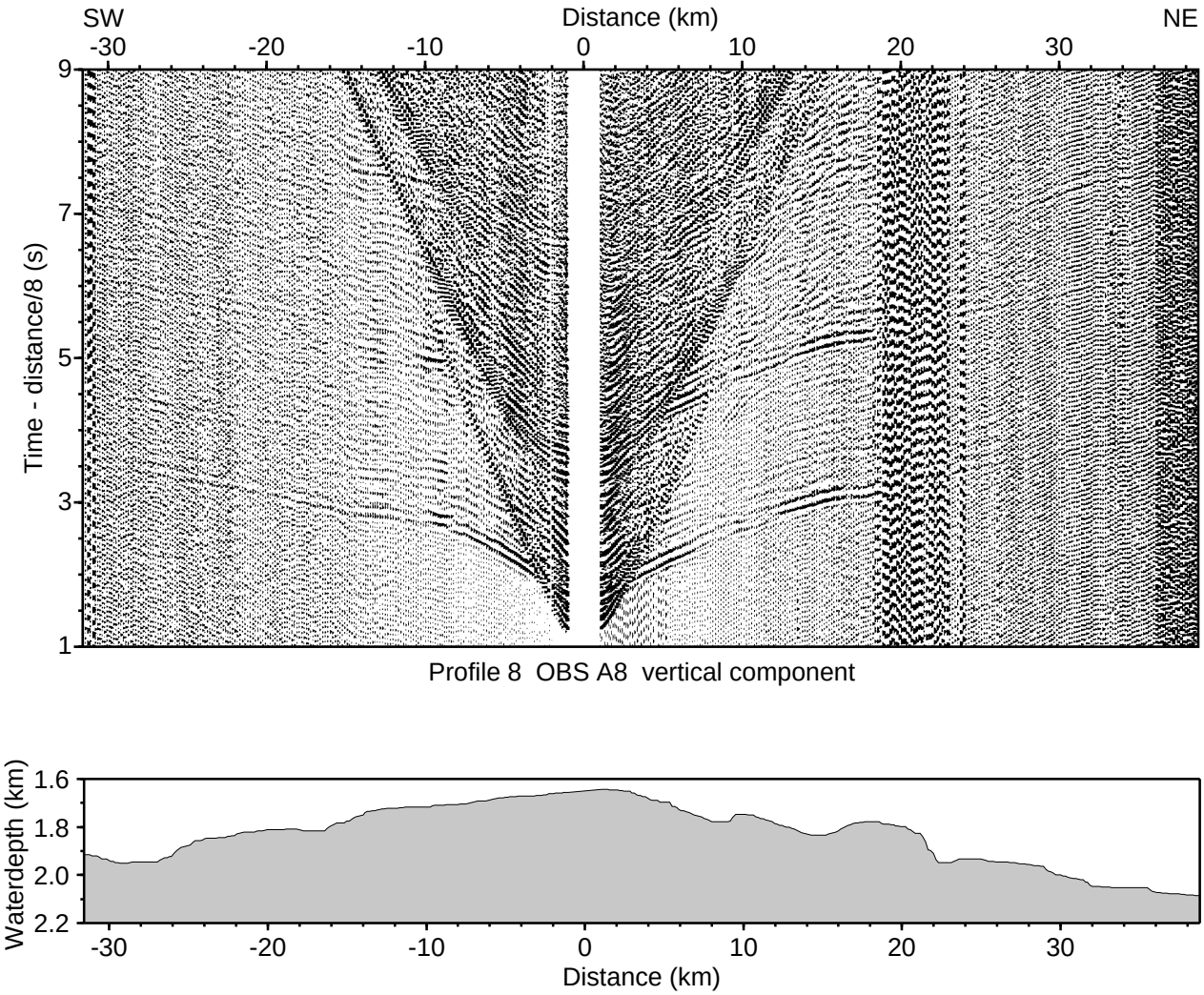

Figure F10 (continued).

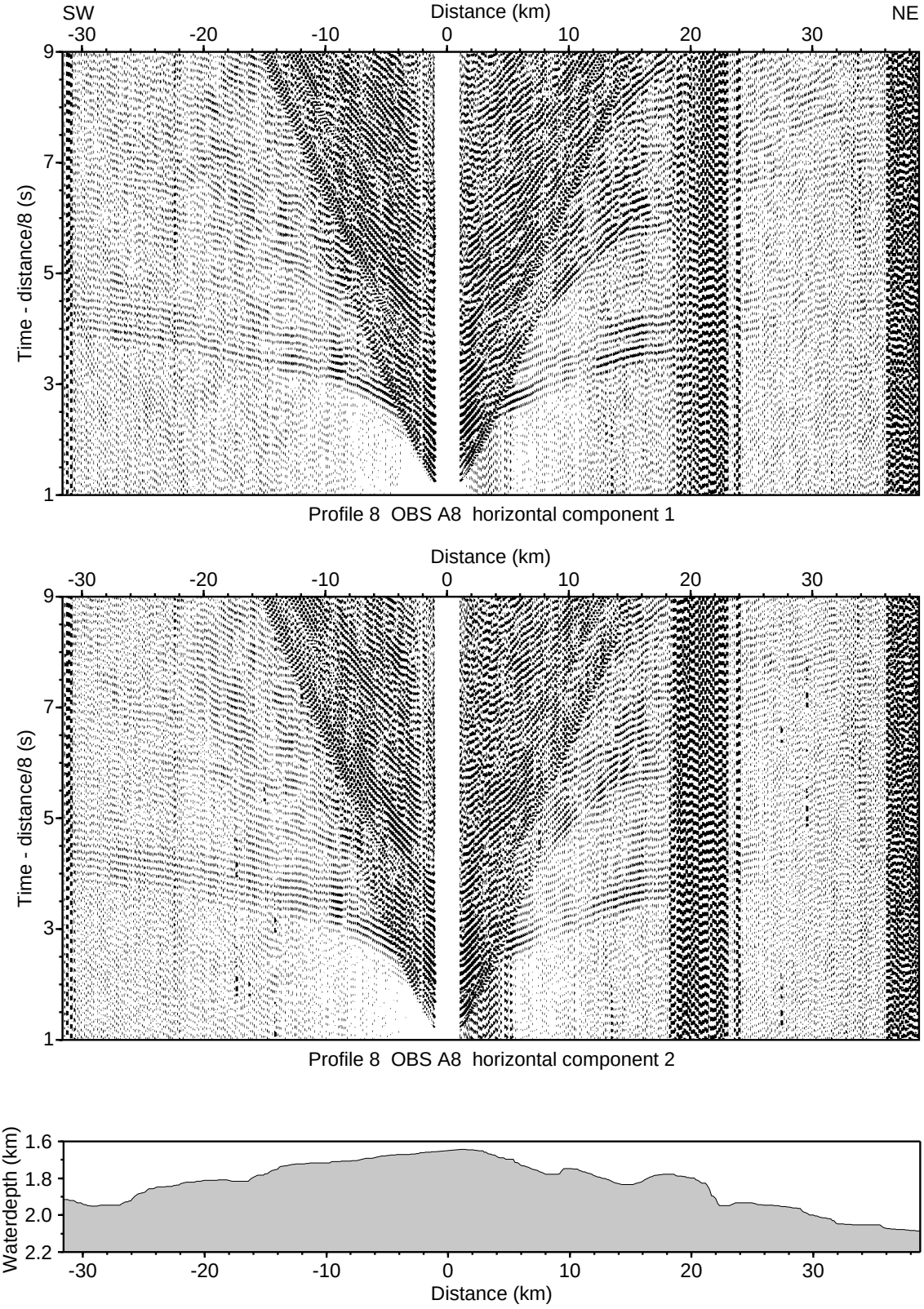

Figure F10 (continued).

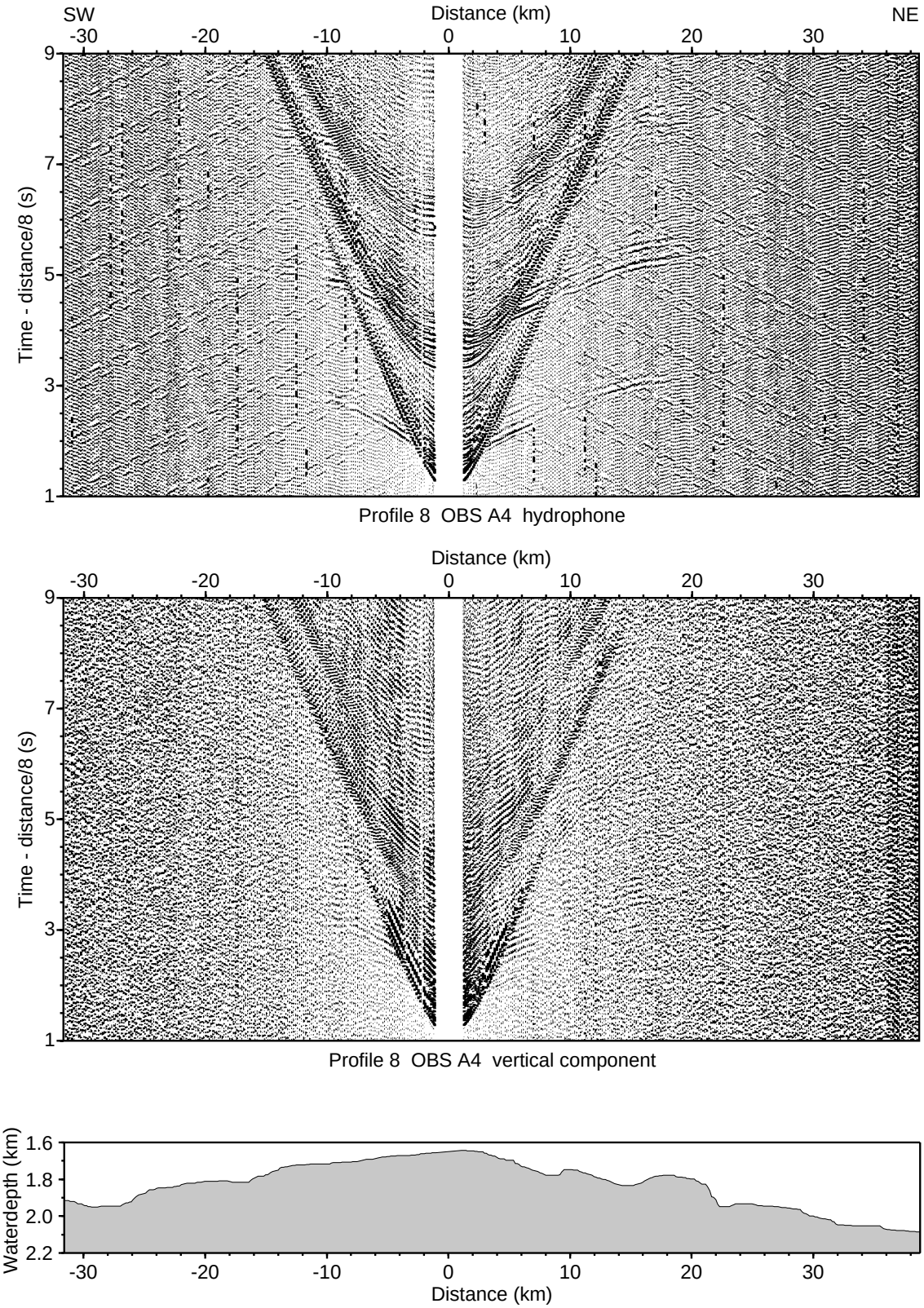

Figure F10 (continued).

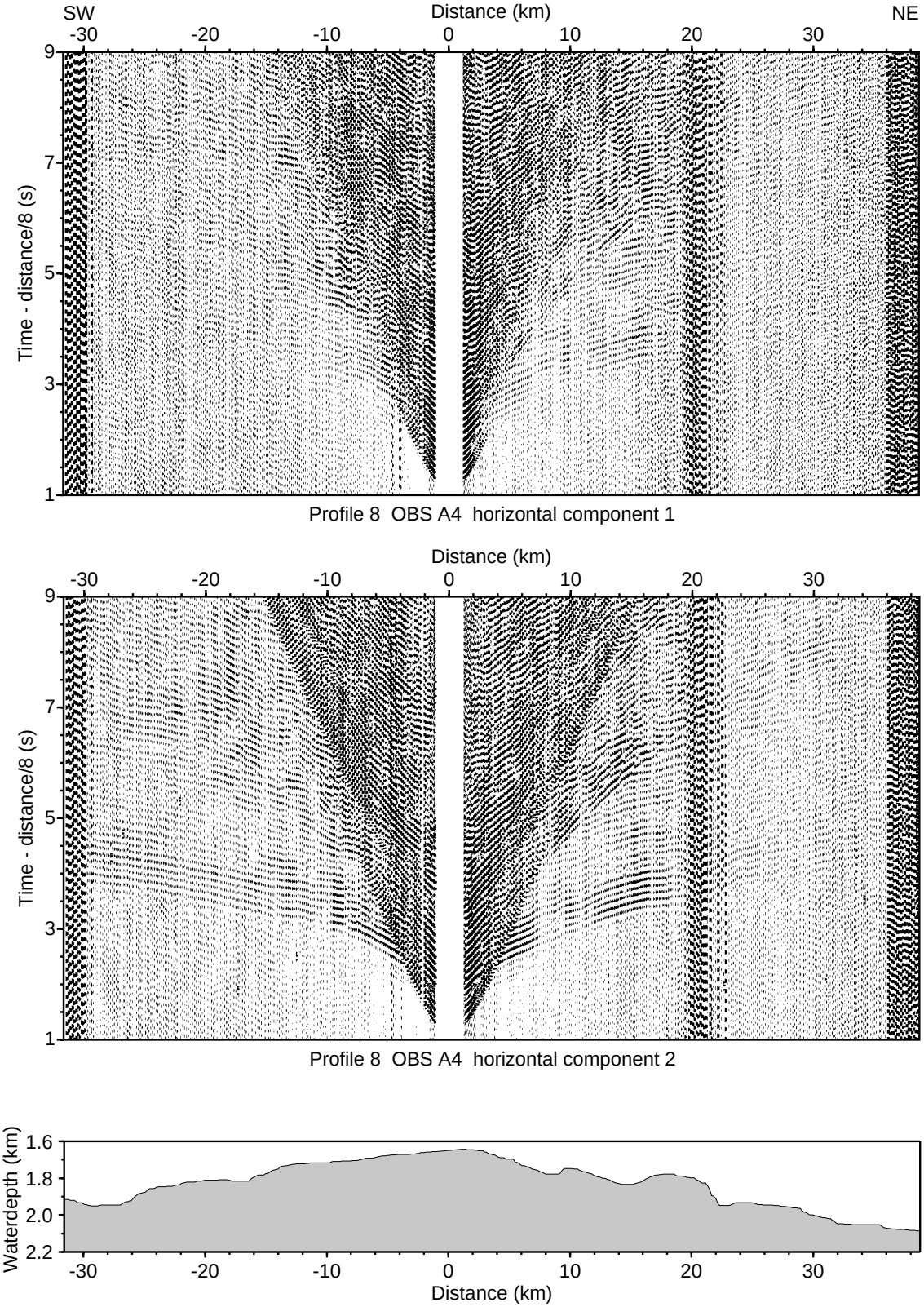

Table T1. Profiles shot by the *Sonne* during OBS deployment.

Line	Date (May 1998)	Time (UTC)	Number of shots	File name
P7	25	0836-1524	409	SO7
P8	26	0156-0432	457	SO8
P9	26	1110-1606	298	SO9
P10	26	1709-2251	343	SOA

Note: Start/end times and number of shots of profiles that were shot by the *Sonne* while the OBSs were deployed from the *Resolution*.